



Self-compacting concrete containing different powders at elevated temperatures – Mechanical properties and changes in the phase composition of the paste

S. Bakhtiyari^a, A. Allahverdi^{b,*}, M. Rais-Ghasemi^c, B.A. Zarrabi^d, T. Parhizkar^c

^a School of Chemical Engineering, Iran University of Science and Technology, Tehran, Iran

^b Cement Research Center, School of Chemical Engineering, Iran University of Science and Technology, Narmak, Tehran 16846-13114, Iran

^c Dep. of Concrete Technology, Building & Housing Research Center (BHRC), Tehran, Iran

^d Fire Technology Dep., SP Technical Research Institute of Sweden, Sweden

ARTICLE INFO

Article history:

Received 14 August 2010

Received in revised form 2 December 2010

Accepted 9 December 2010

Available online 21 December 2010

Keywords:

Self-compacting concrete

Cement paste

Fire resistance

Spalling

Thermal analysis

Quartz powder

ABSTRACT

Fire resistance of self-compacting concretes (SCC) containing limestone and quartz powders, with two different compressive strengths, were evaluated and compared with normal concretes (NC). The residual mechanical strengths of the mixes at different temperatures were measured. The changes in the phase composition of the cement pastes at high temperatures were examined with thermal analysis and X-ray diffractometry methods. The SCC mixes showed a higher susceptibility to spalling at high temperatures but the NC mixes suffered much more from loss of the mechanical strengths. Both the powder types and the compressive strength notably influenced the fire behavior of the SCC. The quartz powder accelerated the hydration of the SCC cement paste at high temperatures, up to 500 °C. However, the quartz-contained SCC showed the highest risk of spalling among all the mixes. The results showed that the thermal analysis could be a useful device for evaluating the fire behavior of building materials.

© 2010 Elsevier B.V. All rights reserved.

1. Introduction

Fire resistance is a property of materials that prevents or retards the passage of excessive heat or flames under conditions of use. For building elements, it is defined as the ability of an element to confine a fire or to continue its structural function, or both, for a stated period of time [1].

Concrete is the most important construction material in the world [2], therefore a lot of experiments have been carried out on fire resistance of traditional concretes. However, the fire behavior of new concretes, like the SCC and high performance concrete (HPC) is very different compared with traditional concretes [3–5].

The SCC was proposed for the first time in 1986 and then developed at the University of Tokyo [6–8]. The SCC fills all sections of forms without the need of mechanical vibration and has reasonable flow-ability, homogeneity, resistance against segregation and mechanical strength [7,9–12]. Use of SCC in the construction industry has been widely growing in almost the entire world and a good growth of use is predicted for it in the near future [13]. Thus,

it is necessary to determine its long-term properties and service performances, such as durability and fire resistance.

The main reasons for failure of a concrete element at high temperatures are spalling and loss of strength. The kind of powder in SCC may significantly affect both of these behaviors. Moreover, the compressive strength of concrete has an important influence on its fire behavior. A higher compressive strength is usually seen with more packing and less porosity, which may lead to higher pore pressures and spalling.

It has been shown that the SCC pastes have different behavior and microstructure at high temperatures relative to the NC and the HPC pastes [14,15]. Boström [16] showed with full scale fire resistance tests that the SCC is more sensitive to spalling relative to NC. The studies on microstructure and phase compositions were not included in his investigation. Boström et al. [18] investigated the effects of size and loading condition on spalling of SCC.

Most research in the field of fire behavior of concrete have focused on the physical and mechanical properties, while the phase composition and the thermal behavior of cement paste have an important role in determining the fire resistance of concrete. Hence, it was needed to investigate these properties to acquire a better perception of the behaviors and to find out the proper solutions for improving the fire behavior of the SCC. Thermal analysis methods can be a very helpful device for this aim.

* Corresponding author. Tel.: +98 21 77240475; fax: +98 21 77240397.

E-mail addresses: bakhtiyari@bhrc.ac.ir (S. Bakhtiyari), ali.allahverdi@iust.ac.ir (A. Allahverdi), raissghasemi@bhrc.ac.ir (M. Rais-Ghasemi), zarrabi@chalmers.se (B.A. Zarrabi), parhizkar@bhrc.ac.ir (T. Parhizkar).

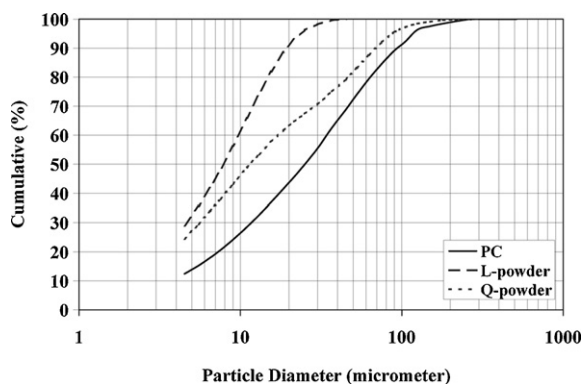


Fig. 1. Cumulative PSD-curves of PC and filling powders.

1.1. Scope

Fire behavior of the SCC containing quartz (Q) and limestone (L) powders (called as Q-specimens and L-specimens hereafter) was investigated. The effects of the compressive strength on the fire resistance of the mixes were evaluated. The silica fume (SF) was used in the high strength concretes as a mineral additive. Two NC mixes were also produced with compressive strength classes similar to the SCC for comparison purposes. The specimens were exposed to high temperatures and then their residual strength and mass were measured. The thermal behavior and phase composition changes of the cement pastes, exposed to different temperatures, were also evaluated with the simultaneous differential scanning calorimetry and thermogravimetry (DSC/TG) and X-ray diffractometry (XRD) tests.

2. Experimental

2.1. Materials

The powders consisted of ASTM-C150 standard type 2 Portland cement (PC), very fine L- and Q-powders. The chemical analysis of the used PC was as following: CaO=61.72, SiO₂=21.18, Al₂O₃=4.10, Fe₂O₃=4.05, MgO=1.20, Na₂O+0.658 K₂O=0.6 and ignition loss=2.9. Using these values in the Bogue's equation, the cement phases were achieved as follows: C₃S=48.43, C₂S=24.19, C₃A=4.01, C₄AF=12.32. The L- and Q-powders with high purity were used as fillers. The chemical analysis showed a purity of more than 97% for both powders. The particle size distribution (PSD) curves of the PC and the filling powders are shown in Fig. 1. Pozzolanic activity of the Q-powder was examined with the thermal analysis method and 27% partial activity was acquired. A commercial ether-carboxylic based product was used as superplasticizer.

Standard aggregates, complied with ASTM C33 were used. The aggregates were of three size fractions, consisting of natural sand (0–4.75 mm), crushed coarse aggregate (4.75–12.5 mm) (gravel 1) and partially crushed coarse aggregate (9.5–19 mm) (gravel 2). The characteristics of the aggregates are presented in Table 1. The chemical analyses were carried out on all three fractions. The results were quite close to each other, showing that the aggregates

Table 1
Characteristics of the used aggregates.

	SSD (g/cm ³)	Dry density (g/cm ³)	Water abs. in SSD (%)	Particles < 75 μm (%)
Sand	2.56	2.49	3.22	1.86
Gravel 1	2.58	2.53	1.99	0.3
Gravel 2	2.57	2.54	1.98	0.25

SSD = surface saturated density.

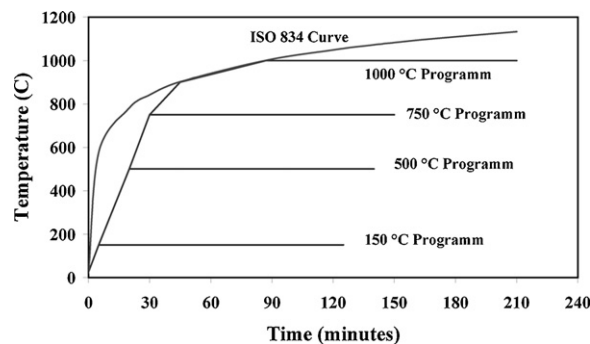


Fig. 2. The used time-temperature programs.

consisted of about 61% SiO₂, 12% Al₂O₃, 9.8% CaO, 8.5% ignition loss, 4.0% Fe₂O₃, 2.0% MgO and 2.7% minor constituents.

2.2. Test methods

2.2.1. Mechanical properties of the hardened concrete

The compressive and the tensile strengths were measured according to EN 12390-3:2000 and ASTM C496 (Brazilian splitting method), respectively. The cubic specimens with 150 mm sides and the cylindrical specimens with diameter of 150 mm × 300 mm height were cast for mechanical tests.

2.2.2. Thermal analysis

DSC/TG tests were performed with a Netsch apparatus, STA 449C, Jupiter. A 10 °C/min temperature rise rate was used for the tests, at atmospheric pressure, in air.

2.2.3. X-ray diffractometry (XRD)

XRD tests were performed by means of a Siemens X-ray diffractometer, using CuK_α radiation generated at 35 kV and 20 mA, in the range of 2θ = 5.0–70.0°.

2.2.4. Fire resistance

The specimens were placed in a laboratory furnace in unloaded condition at four different temperatures, i.e. 150, 500, 750 and 1000 °C. The used time-temperature curves for heating the specimens and the ISO 834 standard fire time-temperature curve are shown in Fig. 2. The specimens were kept in the furnace for 2 h after reaching the target temperature. Then the furnace was turned off and the specimens were left in the furnace for about 24 h in order to reach equilibrium with the ambient temperature. The appearance of the specimens was visually assessed, photographed and then their residual masses and compressive strengths were measured. The spalling behavior of the specimens was also assessed. Two specimens were tested for each mix.

2.3. Specimens casting and curing

Castings of the specimens were carried out according to EN 12390-2:2000. After keeping the specimens at a moist condition for about 24 h, they were demolded and maintained under water

at 23 °C for 7 days. Thereafter, they were kept in a controlled laboratory condition (25 ± 5 °C and $42 \pm 3\%$ humidity) until the tests were performed. This curing regime is similar to the actual conditions of casting of the concrete in Iran, especially for residential building use. Furthermore, if the specimens were kept under water for the entire curing time, the tendency to explosive spalling would have been very high. This viewpoint was also taken into account by other researchers [17–19] for the same reasons.

The paste specimens were cast in $2\text{ cm} \times 2\text{ cm} \times 2\text{ cm}$ molds. These specimens were cured similar to the concrete specimens.

3. Mixtures proportions and the characteristics of samples

3.1. Concrete mixes

The mixtures proportions are given in Table 2. The characteristics of the fresh mixes and the mechanical strengths of the hardened concrete specimens (cured 28 days under water) are presented in Table 3. The SCC and NC codes are used in the table for the self-compacting and the normal-vibrated concrete specimens, respectively.

3.2. Paste compositions

One normal paste including PC and water, and four pastes corresponding to the SCC concretes were made. The pastes were compounded with the same constituents and solids proportions as concrete mixes, without the aggregates and superplasticizer. The water/cement ratios of the pastes were adjusted to achieve normal consistency. The following notations are used in the paper for the tested pastes: NCP-4 for normal paste, SCCP-S4 and SCCP-S5 for SCC pastes containing the Q-powder and the SF mineral additive, and SCCP-C4 and SCCP-C5 for the SCC pastes containing the L-powder.

4. Results and discussion

4.1. Thermal analysis of powders

For a better assessment of the effects of thermal behavior of the used powders on the fire behavior of the concretes, DSC/TG tests were performed on the powders. The results are presented in Fig. 3.

Table 2
Proportions of mixes.

Code	PC (kg/m ³)	SF (kg/m ³)	CA (kg/m ³)		FA (kg/m ³)		P (kg/m ³)	Powder type	W (kg/m ³)	SP (% of PC)
			4.75–12.5 (mm)	12.5–19 (mm)	0–2 (mm)	0–5 (mm)				
SCC-S4	320	0	313	313	306	715	185	Quartz	175	1.35
SCC-S5	372	28	312	317	301	728	120	Quartz	160	1.55
SCC-C4	320	0	313	313	306	715	185	Limestone	175	0.88
SCC-C5	372	28	312	317	301	728	120	Limestone	160	0.85
NC-4	350	0	409	415	282	700	–	–	175	0.75
NC-S5	372	28	405	413	290	703	–	–	160	0.38

PC = Portland cement; SF = silica fume; CA = coarse aggregate; FA = fine aggregate; P = powder content; W = water content; SP = super-plasticizer.

Table 3
Characteristics of the fresh and hardened SCC mixes.

Code	SLF (mm)	T_{500} (s)	h_2/h_1 in box test	V fl. time (s)	V funnel T5 (s)	Sp. gr. (kg/m ³)	28-Day comp. st. (MPa)		28-Day tensile st. (MPa)
							Cube	Cylind.	
SCC-S4	640	2.0	0.84	4.0	4.0	2265	41.0	31.2 ± 1.0	3.5 ± 0.2
SCC-S5	670	2.2	0.89	4.0	5.5	2338	52.2	41.8 ± 0.8	3.7 ± 0.7
SCC-C4	710	1.0	0.85	3.5	4.0	2290	40.4	29.7 ± 0.6	3.2 ± 0.1
SCC-C5	630	1.5	0.85	4.0	4.0	2310	52.6	39.7 ± 0.3	3.4 ± 0.2
NC-4	19	–	–	–	–	2347	34.5	25.5 ± 0.5	2.8 ± 0.1
NC-S5	7.5	–	–	–	–	2300	59.0	38.0 ± 0.1	4.2 ± 0.1

SLF = slump flow (or slump for the traditional vibrated mixes); V fl. = V funnel flowing time; Sp. gr. = specific gravity; cylind. = cylindrical.

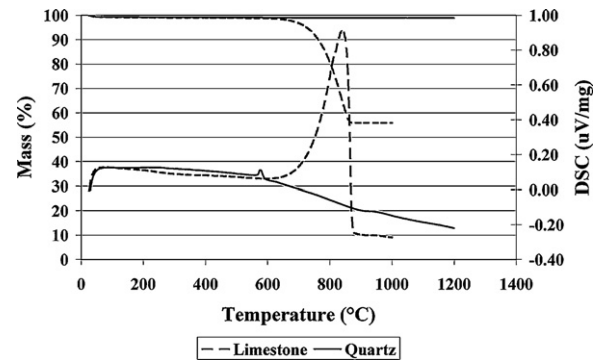


Fig. 3. DSC/TG curves of limestone and quartz powders.

The mass of the Q-powder was almost constant up to 1200 °C, indicating that it did not decompose with temperature. The peak at 576.2 °C and the slope change at 893 °C on the DSC curve of the Q-powder are related to the changes of the crystalline structure of quartz from α to β and from β -quartz to tridymite, respectively.

The TG curve of calcium carbonate showed 43% weight loss, which starts at about 650 °C and continues up to about 860 °C. The peak of 841 °C on DSC curve of calcium carbonate is related to decomposition of CaCO_3 to CaO and CO_2 .

4.2. Residual strength and mass loss of the concrete specimens at high temperatures

The results of residual compressive strength ($f_{c,res}$) and mass loss of specimens tested at high temperatures are presented in Table 4. The indexes at the end of the names of the specimens in the table show the test temperature (e.g. SCC-S4-500 means the SCC containing the Q-powder; 40 MPa compressive strength class; tested at 500 °C). Two specimens were tested for each mix at each temperature and the average was reported. The reported compressive strength of the control samples represents the average of 3 specimens, cured for 28 days in conditions similar to the fire test specimens.

The curves of the average relative residual strengths of the mixes versus temperature are presented in Fig. 4.

Table 4

The average residual strength and the average mass loss of the concrete specimens after fire resistance test.

Code	$f_{c,25}$, av. (MPa)	$f_{c,res}$, av. (MPa)	Change of comp. st., av., (%)	Mass loss, av. (%)	No. of spalled specimens
SCC-S4-150	43.2 ± 1.1	44.3 ± 0.1	2.5	1.75 ± 0.1	–
SCC-S4-500		51.3	18.8	6.4	1
SCC-S4-750		–	–	–	–
SCC-S5-150	56.3 ± 0.3	53.4 ± 3.0	–5.2	1.78 ± 0.03	–
SCC-S5-500		76.7 ± 2.1	36.2	6.1 ± 0.3	–
SCC-S5-750		Explos. Spall.	–	–	–
SCC-C4-150	42.4 ± 0.9	37.8 ± 0.4	–10.8	2.0 ± 0.07	–
SCC-C4-500		37.2 ± 0.8	–12.3	5.5 ± 0.2	–
SCC-C4-750		17.3	–59.2	7.42	1
SCC-C5-150	55.3 ± 0.8	47.5 ± 0.8	–14.1	1.93 ± 0.07	–
SCC-C5-500		49.0 ± 2.5	–11.4	5.84 ± 0.08	–
SCC-C5-750		17.9 ^a	–67.6	8.3	–
NC4-150	35.9 ± 0.3	29.5 ± 0.1	–17.8	2.6 ± 0.1	–
NC4-500		27.0 ± 1.9	–24.8	5.9 ± 0.1	–
NC4-750		7.6	–79.9	7.6	1
NC4-1000		3.1 ± 0.0	–91.4	12.3	–
NC-S5-150	62.0 ± 0.2	52.4 ± 1.7	–15.5	1.93 ± 0.0	–
NC-S5-500		47.8 ± 4.0	–22.9	6.4 ± 0.2	–
NC-S5-750		18.6 ± 0.1	–70	8.1 ± 0.3	–
NC-S5-1000		5.9 ± 0.4	–90.5	12.7 ± 0.1	–

$f_{c,25}$ = compressive strength of control specimens at 25 °C; $f_{c,res}$ = residual compressive strength; comp. st. = compressive strength; explos. spall. = explosive spalling; a: only one specimen could be tested.

4.2.1. Influence of the powder type on fire resistance of the SCC

The effect of the temperature on the compressive strength of the Q-specimens was negligible at 150 °C, but significant at 500 °C. One of the SCC-S4 specimens explosively spalled at 500 °C. On the other hand; the second specimen of the same mix did not spall and showed an 18% increase in the compressive strength. This should be because that the partial pozzolanic activity of the Q-powder could be enhanced at high temperatures and in the presence of water vapor, which produced an internal autoclaved condition and accelerated the strength development.

A different behavior was observed from the Q-specimens of the class 50 MPa. The Q-specimens did not spall at 500 °C and their relative residual strength was considerably higher than those of class 40 MPa specimens. The reason could be the simultaneous existence of Q-powder and SF. The pozzolanic activity brought about by Q-powder and SF was much more effective than Q-powder alone. SF improves the strength of the transition zone between paste and aggregates [20,21]. Moreover, the quality of the transition zone in the SCC is significantly better than that of the NC [21]. It can be expected that these phenomena together (accelerated hydration and improved transition zone) resulted in the higher tensile strength, which could overcome the pore pressure and thermal stresses produced at high temperatures. Hence, the higher tensile strength of 50 MPa specimens should be the reason they showed a better resistance-to-spalling at 500 °C in comparison to 40 MPa specimens.

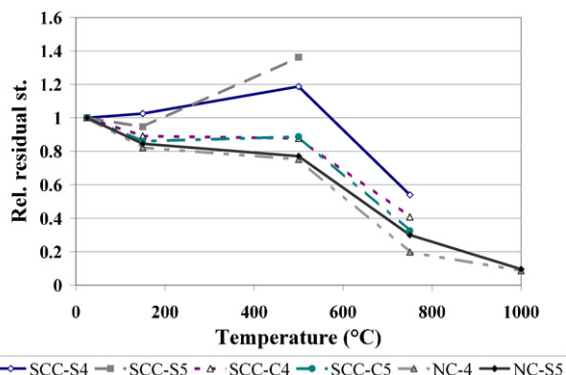


Fig. 4. Relative residual compressive strength of SCC and NC mixes vs. temperature.

All four Q-specimens spalled at 750 °C. The spalling of the SCC-S5 specimens was highly explosive and caused damage to the furnace.

The L-specimens showed a different behavior compared to the Q-specimens. Their residual compressive strength did not increase with temperature. However, the strength losses were not significant up to 500 °C. No spalling occurred at 500 °C. One specimen showed a corner type spalling at 750 °C. Their average relative residual strength at 750 °C was considerably less than that of the Q-specimens.

Based on the TG results (Fig. 3), about 9% of the mass of L-powder was lost at 750 °C. Theoretically, this could result in increased pore volumes and decreased pore pressure, which counteracts spalling of the concrete.

Assessment of the mass loss of the specimens did not rise to an obvious relation between the mass loss and the fire behavior of the specimens.

4.2.2. Influence of type of concrete (SCC and normal traditional vibrated)

The NC specimens did not suffer from spalling. However, their strength losses were significantly more than those of the SCC specimens were. The results showed that if spalling of the SCC can be controlled, the residual strength of SCC is higher than NC.

Kalifa [22] showed that the spalling of concretes can be controlled with use of polypropylene fibers. The improvement of spalling behavior of concretes may be also done with replacement of a part of the aggregates with natural or synthetic lightweight aggregates. This will be investigated in the further stages of this research project.

4.2.3. Influence of the compressive strength

Comparison of the 40 and 50 MPa Q-specimens at 500 °C showed that the 50 MPa specimens gained about 36% increase of strength; i.e. about two times the 40 MPa ones. Despite the expectation that the risk of spalling would increase by compressive strength [4,23–25], the 50 MPa specimens did not spall at 500 °C. The pozzolanic activities of the Q-powder and SF and the increased residual tensile strength of the concrete at 500 °C may be the reasons of this improved fire resistance. Ali [26] observed similar behavior in his experiments on concrete columns and proposed that the higher splitting tensile strength was the reason for better resistance-to-spalling of the mixes with the higher compressive strength. The

measurement of the tensile strengths of the specimens was not performed in his research.

Both 40 and 50 MPa Q-specimens spalled at 750 °C. The severity of spalling of 50 MPa specimens was considerably higher and the specimens were crushed into many pieces. The reasons should be the less pore content in 50 MPa specimens and the subsequent increased pore pressure.

The behaviors of the L-specimens of both compressive strength classes were similar. No explosive spalling occurred for them.

Behavior similar to the L-specimens was observed for the NC concretes, with the difference that no spalling occurred for the NC specimens and their relative strength loss were more than the SCC mixes.

4.2.4. Residual tensile strength

It appeared that the residual tensile strength had a significant role in the spalling of concrete. Hence, it was attempted to perform tensile tests on the available specimens. The SCC-S4 was remixed for this purpose. A high strength SCC containing Q-powder, cured at the same conditions, was also available in the laboratory. Its composition was similar to SCC-S5, but with less water/cement ratio. As the specimens were susceptible to spalling at 500 °C, the tests were carried out at 350 °C. However, the SCC-S7 specimen explosively spalled even at this temperature. Thus the fire test was repeated at 250 °C. The results are presented in Table 5.

The ratios of the tensile to the compressive strengths were approximately constant at tested temperatures. This is in agreement with the idea given in the above sections about the relation between spalling and tensile/compressive strengths of the mixes. However, it is expected that the tensile strength is decreased faster than the compressive strength at higher temperatures, due to the characteristics of the transition zone between the paste and the aggregates [2]. Phan [4] reported a maximum pore pressure of 2.1 MPa before spalling of a 98 MPa HSC specimen (compare with the tensile results in Table 5).

Severe explosive spalling of the SCC-S7 at 350 °C showed that very high strength SCC is highly sensitive to spalling, even at temperatures of early stages of fire.

Table 5

The residual tensile and compressive strengths for two SCC-S mixes.

Code	Temperature (°C)	Comp. st. (MPa)	Tensile st. (MPa)	Tens. st/comp. st. ratio
SCC-S4-R	25	45.51	2.39	0.053
	350	61.45	3.40	0.055
SCC-S7	25	70.11	2.88	0.041
	250	86.7	3.51	0.040
	350	Explosive spalling		

Table 6

The average residual compressive strength, the mass loss and the shrinkage of the specimens after exposure to high temperature.

Code	$f_{c,25}$ (MPa)	$f_{c,res}^T$ (MPa)	Change of comp. st. (MPa)	Mass loss (%)	Shrinkage (%)
NCP-4-500		90.58 ± 1.94	2.54	13.66 ± 0.05	-1.3
NCP-4-750	88.34 ± 11.72	33.57 ± 0.87	-62.00	15.19 ± 0.05	-1.5
SCCP-S4-500		56.79 ± 3.82	-9.57	10.42 ± 0.19	-0.7
SCCP-S4-750	62.8 ± 6.07	30.09 ± 0.87	-52.09	12.59 ± 0.46	-1.0
SCCP-S5-500		80.73 ± 7.76	-1.18	13.57 ± 0.35	-1.2
SCCP-S5-750	81.69 ± 1.47	54.94 ± 2.52	-32.75	16.09 ± 0.35	-1.7
SCCP-C4-500		50.35 ± 3.00	-21.39	10.45 ± 0.20	-0.7
SCCP-C4-750	64.05 ± 3.45	18.64 ± 1.46	-70.90	22.19 ± 0.33	-1.5
SCCP-C5-500		78.42 ± 2.03	-1.86	14.02 ± 0.55	-1.4
SCCP-C5-750	79.91 ± 3.92	21.99 ± 2.65	-72.48	22.3 ± 0.44	-2.3

$f_{c,res}^T$ = average residual compressive strength at t temperature (after cooling), $f_{c,25}$ = control compressive strength at ambient temperature, av. = average.

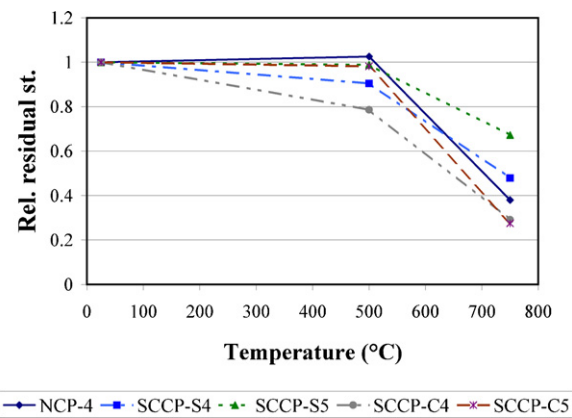


Fig. 5. The relative residual compressive strength of the cement pastes at 500 °C and 750 °C.

4.3. The residual compressive strength and the physical changes of the cement pastes at high temperatures

The residual compressive strengths of the cement paste specimens after exposure to 500 °C and 750 °C are presented in Table 6, accompanied with the mass losses and the thermal shrinkage. The relative residual strength of the specimens is illustrated in Fig. 5. The thermal shrinkage of the specimens consists of both the drying shrinkage and the thermal contraction of the specimens. The separate measurement of these two shrinkages is not possible [27].

4.3.1. Residual compressive strength

The changes of compressive strength of the normal paste and the SCC pastes containing SF (SCCP-S5 and SCCP-C5) were very small at 500 °C; see Table 6 and Fig. 5. Hence, the existence of SF in the composition could be the reason of the better residual compressive strengths of the S5 and C5 pastes at temperatures up to 500 °C.

The lowest residual compressive strength was related to the L-specimens at 750 °C. The high content of L-powder in these specimens is most likely the reason of this behavior.

The Q-specimens showed the highest residual compressive strength among all the specimens at 750 °C. It may be due to the partial pozzolanic effect of the Q-powder and the improvement in quality of the hydrated pastes.

4.3.2. Mass loss and thermal shrinkage

An assessment of the mass loss data did not produce any additional information. The thermal shrinkage data is presented in Table 6. The strength loss of specimens at high temperatures did not show any particular relation with shrinkage.

4.4. Phase composition and structure changes

The phase composition and the structure changes of hardened normal and SCC pastes were examined with XRD and DSC/TG tests. The results are presented and discussed in the following.

4.4.1. XRD

The normal and SCC pastes, including NCP-4, SCCP-S4, SCCP-S5 and SCCP-C4, exposed to ambient and high temperatures (500 °C and 750 °C), were examined with XRD. The heating procedure of these specimens was similar to concrete ones. After natural cooling of the specimens to reach equilibrium with room temperature, they were crushed and sieved to achieve a proper specimen for XRD. The XRD results are presented in Fig. 6. The graphs are shown at 2θ angles between 20° and 40° that contain the most important peaks of the cement and the powders. The following notations are used in the graphs: CH=Ca(OH)₂, C_nS=C₂S and C₃S, CC=CaCO₃, CO=CaO, S=SiO₂.

Fig. 6a shows a small increase in the C_nS amount and considerable decomposition of Ca(OH)₂ at 500 °C, while CaCO₃ is almost constant and unchanged at this temperature. The peaks related to Ca(OH)₂ and CaCO₃ almost completely disappeared at 750 °C, indicating that these compounds were almost entirely decomposed after 2 h exposure at this temperature. Meanwhile, the related peaks of C_nS and CaO showed a considerable increase at 750 °C, indicating the decomposition of C–S–H gels and CaCO₃, respectively.

In SCCP-S4 graphs (Fig. 6b) a distinguished peak of SiO₂ was observed at $2\theta = 26.7^\circ$. The value of peak slightly decreased at 500 °C indicating that part of SiO₂ entered in the hydration reaction due to its pozzolanic activity. The peak values of Ca(OH)₂ and C_nS also decreased due to hydration reactions.

In SCCP-S5 graphs (Fig. 6c), the peak of quartz at $2\theta = 26.7^\circ$ decreased at 500 °C and then increased again at 750 °C. This demonstrated that SiO₂ was in the hydration reactions at 500 °C due to its pozzolanic effect, but subsequently was released again at 750 °C because of decomposition of C–S–H. Decreasing and increasing of C_nS at 500 °C and 750 °C agreed with this explanation.

The XRD graphs of SCCP-C4 are presented in Fig. 6d. It contained large amount of CaCO₃ with a sharp peak at $2\theta = 29.5^\circ$. The amount of CaCO₃ significantly decreased at 750 °C, due to its partial decomposition at this temperature. The peak of CaO was very small at 500 °C, but very distinguished at 750 °C, which was due to decomposition of CaCO₃ to CaO and CO₂. The amount of Ca(OH)₂ increased again at 750 °C which could be due to large amounts of CaO in the solid paste and its reaction with moisture during the cooling period.

Increase of C_nS at 750 °C, observable in graphs of all specimens, was a result of decomposition of the cement gels. Examining the XRD results, decomposition of C–S–H must occur at temperatures higher than 500 °C. Peng [28] studied decomposition of the hardened cement pastes, exposed to different temperatures, by XRD method. He mentioned that the decomposition of C–S–H started at 600 and completes at 800 °C. However, no obvious peak of C–S–H was found in this study and other researches [29–31], because it is an amorphous or cryptocrystalline material and its crystalline

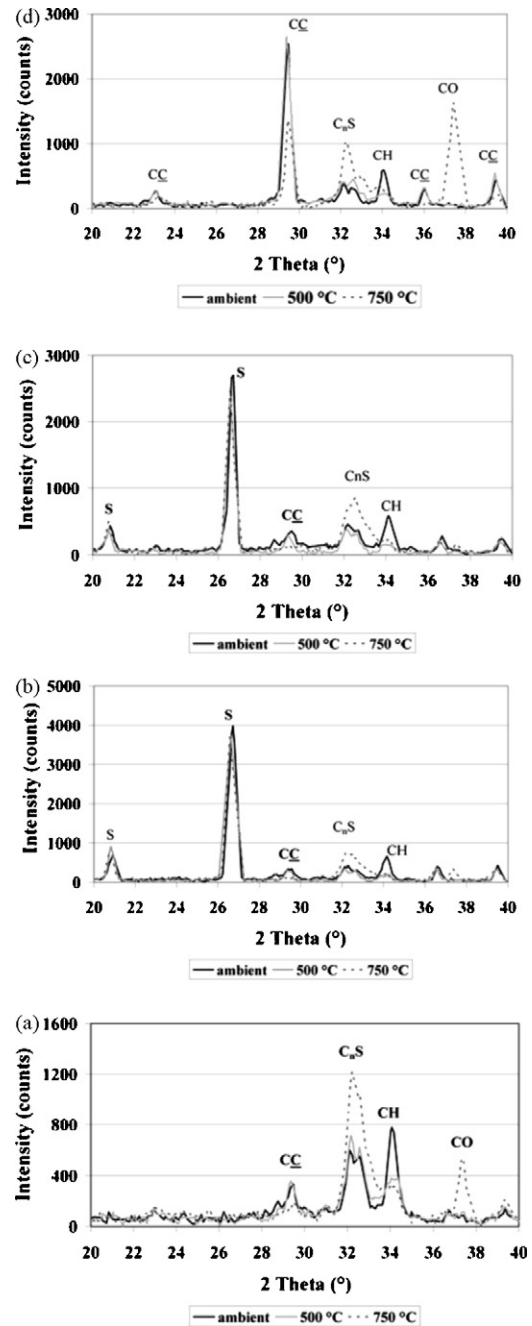


Fig. 6. XRD graphs for the pastes at 25, 500 and 750 °C: (a) NCP-4, (b) SCCP-S4, (c) SCCP-S5, (d) SCCP-C4.

content is not sufficient to give a sharp peak in XRD tests. Stepkowska et al. [32] also did not assign a particular peak to C–S–H and instead used the variations of peaks of alite, belite and CaO for assessing the C–S–H variations.

It is considerable that for the specimens exposed to high temperatures, the C_nS peak was much sharper for the normal and the limestone-contained SCC pastes in comparison to the quartz-contained SCC pastes. In other words, the amount of decomposition of the C–S–H was much higher in the normal and the L-specimens in comparison to the Q-specimens. It can be concluded that the quality of chemical bonds in the C–S–H gels of the quartz-contained SCC mixes should be better than the other ones. This should be due to the partial pozzolanic activity of the Q-powder, which decreases Ca(OH)₂ and increases the C–S–H content. This description can explain the reasons of the higher relative strength of the quartz-

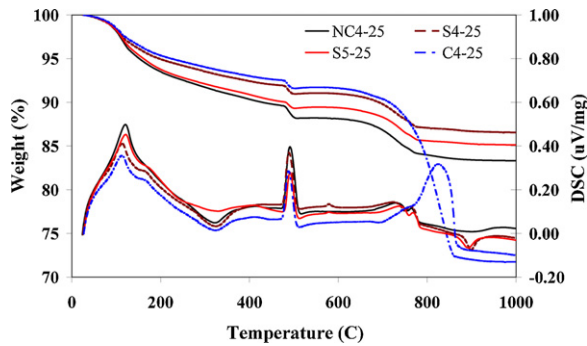


Fig. 7. DSC/TG curves for paste specimens at 25 °C.

contained SCC relative to the other mixes, from the viewpoint of phase composition.

4.4.2. Thermal analysis

The main parameters of fire resistance are stability and integrity. The failure of these parameters is generally occurred because of changes in composition and structure of the element. The thermal analysis methods, like DSC and TG can be helpful for evaluating these changes and can be used for predicting the fire behavior of materials or as supportive data for interpretation of the results. In this investigation, we examined this capability for interpretation of residual mechanical test results.

DSC/TG tests were performed on normal and SCC cement pastes, including NCP-4, SCCP-S4, SCCP-S5 and SCCP-C4. They were cured similar to the concrete samples. Two series of paste specimens with an age of 28 days were exposed to 500 °C and 750 °C in accordance with the temperature–time curves presented in Fig. 2. After natural cooling, the specimens were crushed and powdered, so that suitable specimens were prepared for the DSC/TG tests. The results of DSC/TG measurements are depicted in Figs. 7–9.

The first peak on the DSC curve of NC4-25 was seen at 122 °C, corresponding to the decomposition of ettringite and the loss of physical water. A mass loss of about 7% was observed at 200 °C, which relates to the release of surface water, C–S–H gels and ettringite water. The TG curve continued with a smooth slope to about 482 °C. The continuous decrease of the weight of the specimen indicates partial release of the chemical bounded water from various complex hydrated compounds, [31–34]. The total weight of the lost water was 10.5% up to 480 °C.

The peak at 491 °C on the DSC curve of NC4-25 corresponds to decomposition of Portlandite [31–34]. The decomposition started from 480 °C and continued to around 507 °C. Two peaks were observed on the DSC curve at 735 °C and 764 °C. Both of these peaks have been assigned to decomposition of carbonates, the first one to the amorphous calcium carbonate and the second to the well crystallized calcite [30,33].

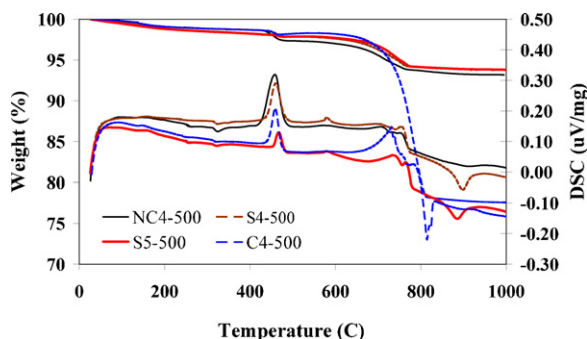


Fig. 8. DSC/TG curves for paste specimens at 500 °C.

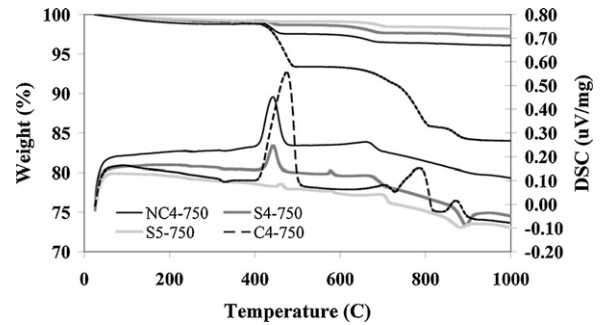


Fig. 9. DSC/TG curves for paste specimens at 750 °C.

No considerable mass loss was seen on TG curves of NC4-500 and NC4-750 specimens up to 420 °C. Their DSC curves also showed an almost stable condition up to this temperature. This behavior is because of the thermal history of these specimens. The mass loss related to the decomposition of Portlandite was still observed for both of these specimens, illustrating reversible nature of decomposition of $\text{Ca}(\text{OH})_2$.

The mass loss due to the decomposition of Portlandite was very close in all specimens with regard to the content of the cement. The SCCP-S5 was an exception, in which the mass loss due to Portlandite decomposition was much less than the other specimens. The reason could be the presence of SF in the S5 formulation. SF could react with Portlandite, and produce more gel compounds. The weakened peaks of Portlandite on the DSC curves of SCCP-S5-500 and SCCP-S5-750 specimens agree with the discussions presented in the previous sections about the improved pozzolanic activity of Q-powder and SF at high temperatures. The same behavior was observed and reported by other researchers [34 and references 11–13 in it].

Evaluation of the DSC/TG curves revealed that the tested pastes had almost constant mass and stable structural state between 450 °C and 650 °C. In other words, it may be expected that the pore volumes will not increase much in this temperature range, except due to probable development of the microcracks because of the thermal movement. As a result, the pore pressure will rise with temperature. At the same time, the molecular bonds became weaker with the rise of temperature, because of higher energy levels of the particles and increased kinetic movements. This means weaker adhesion ability of the hardened paste and hence, decreased mechanical strength of the concrete. Therefore, it can be stated that is more possible in this temperature range for the pore vapor pressure to overcome residual tensile strength, resulting in the spalling. This explanation agrees with the observed behavior of the SCC specimens at 500 °C and 750 °C.

5. Conclusions

1. With considering the test results and observations, it can be said as a general rule that 500 °C is a critical temperature for concretes exposed to fire. Considering a proper safety factor for the loadbearing elements, the loss of strength is not critical before this temperature. The significant loss of the compressive strength of the concrete mixes at higher temperatures is mainly due to decomposition of the cement paste and significant loss of adhesion.
2. The DSC/TG results of cement pastes revealed that temperatures of 480–650 °C could be the most dangerous temperature range for the occurrence of spalling in concretes.
3. The results showed that the thermal analysis methods are useful for evaluation in the fire behavior of materials or as supportive data for interpretation of the fire test results.

4. The self-compacting concretes (SCC) are more susceptible to spalling than the normal vibrated concretes (NC). However, the relative residual strength of the NC falls considerably faster than the SCC at high temperatures.
5. If fine quartz powder is used as filler in the SCC, it will accelerate the strength development at high temperatures up to 500 °C, because of its partial pozzolanic activity, enhanced at such temperatures. Such an effect could result in increased pore pressure and therefore a higher risk of spalling of the concrete. The significant weak point of the quartz-contained SCC at elevated temperatures is spalling and for the limestone-contained SCC, the loss of the adhesion ability in the cement paste is a disadvantage. The effects of the age, the moisture content and the curing condition on fire resistance of the SCC need to be investigated.
6. Most of the research on the fire behavior of concretes has been carried out on the residual compressive strength. It was revealed that the residual tensile strength is very significant in this regard and should be considered during investigations.

Acknowledgments

The Building and Housing Research Center (BHRC) provided financial and laboratory supports for this research. The technical committee of concrete technology supervised on the progress of the research. In this regard, the valued comments of Professor A. A. Ramezani pour and Dr. P. Ghodusi should be acknowledged. The authors also appreciate the cooperation of the members of steering committee of the PhD thesis at Iran University of science and technology. The authors also wish to appreciate Mrs. F. Jafarpour and Miss F. Firoozyar for performing DSC/TG tests and all the staff of the concrete laboratory of BHRC for their valued cooperation during this project.

References

- [1] BS EN ISO 13943:2000, Fire Safety – Vocabulary, British Standard Inst., London, 2000.
- [2] P.K. Mehta, D.J.M. Monterio, *Concrete: Microstructure, Properties and Materials*, third ed., McGraw Hill Book Company, 2006.
- [3] Y. Anderberg, Spalling phenomena of HPC and OC, in: L.T. Phan (Ed.), *Proceedings of the International Workshop on Fire Performance of High Strength Concrete*, NIST, Maryland, 1997, pp. 69–75.
- [4] L.T. Phan, High strength concrete at high temperature – an overview, in: F.G. Dehn, T. Faust (Eds.), *Proceedings of the Sixth International Symposium of Utilization of High Strength/High Performance Concrete*, vol. 1, Leipzig, 2002, pp. 501–518.
- [5] C.M. Aldea, Fire tests on normal and high-strength reinforced concrete columns, in: L.T. Phan (Ed.), *Proceedings of the International Workshop on Fire Performance of High Strength Concrete*, NIST, Maryland, 1997, pp. 109–124.
- [6] H. Okamura, M. Ouchi, Self-compacting high performance concrete, *Prog. Strut. Eng. Mater.* 1 (1998) 378–383.
- [7] H. Okamura, M. Ouchi, Self-compacting concrete, *J. Adv. Concr. Technol.* 1 (2003) 5–15.
- [8] P.J.M. Bartos, M. Grauers, Self-compacting concrete, *Concrete* 33 (1999) 9–13.
- [9] W. Zhu, J.C. Gibbs, P.J.M. Bartos, Uniformity of in situ properties of self-compacting concrete in full scale structural elements, *Cem. Concr. Comp.* 23 (2001) 57–64.
- [10] K. Ozawa, K. Maekawa, M. Kunishima, H. Okamura, Development of high performance concrete based on the durability design of concrete structures, in: *Proceedings of the Second East-Asia and Pacific Conf. on Struct. Eng. Constr. (EASEC-2)*, vol. 1, 1989, pp. 445–450.
- [11] P.L. Domone, Self-compacting concrete: an analysis of 11 years of case studies, *Cem. Concr. Comp.* 28 (2006) 197–208.
- [12] P.L. Domone, A review of the hardened mechanical properties of self-compacting concrete, *Cem. Concr. Comp.* 29 (2007) 1–12.
- [13] M. Ouchi, S. Nakamura, Th. Osterberg, S. Hallberg, M. Lwin, Applications of Self-compacting Concrete in Japan, Europe and The United States, US Dep. of transportation, Fed. Highway Adm., 2006, www.fhwa.dot.gov/bridge/scc.htm.
- [14] G. Ye, X. Liu, G. De Schutter, L. Taerwe, P. Vandeveld, Phase distribution and microstructural changes of self-compacting cement paste at elevated temperature, *Cem. Concr. Res.* 37 (2007) 978–987.
- [15] G. Ye, X. Liu, G. De Schutter, A.M. Poppe, L. Taerwe, Influence of limestone powder used as filler in SCC on hydration and microstructure of cement pastes, *Cem. Concr. Res.* 29 (2007) 94–102.
- [16] L. Boström, The Performance of Some Self Compacting Concretes When Exposed to Fire, SP Report 2002:23, SP Swedish National Testing and Research Inst., 2002.
- [17] B. Persson, Fire resistance of self-compacting concrete, SCC, *Mater. Struct.* 37 (2004) 575–584.
- [18] L. Boström, U. Wickström, B.A. Zarrabi, Effect of specimen size and loading conditions on spalling of concrete, *Fire Mater.* 31 (2007) 173–186.
- [19] Rilem draft recommendation-129-MHT test methods for mechanical properties of concrete at high temperatures, *Mater. Struct.* 28 (1995) 410–414.
- [20] A. Leeman, B. Münch, P. Gasser, L. Holzer, Influence of compaction on the interfacial transition zone and the permeability of concrete, *Cem. Concr. Res.* 36 (2006) 1425–1433.
- [21] K.L. Scrivener, A. Bentur, P.L. Pratt, Quantitative characterization of the transition zone in high strength concrete, *Adv. Cem. Res.* 1 (1988) 230–237.
- [22] P. Kalifa, High-temperature behavior of HPC with polypropylene fibers: from spalling to microstructure, *Cem. Concr. Res.* 31 (2001) 1487–1499.
- [23] K.D. Hertz, Limits of spalling of fire exposed concrete, *Fire Saf. J.* 38 (2003) 103–116.
- [24] C. Castillo, A.J. Durrani, Effect of transient high temperature on high-strength concrete, *ACI Mater. J.* 87 (1990) 47–53.
- [25] L.T. Phan, N.J. Carino, Review of mechanical properties of HSC at elevated temperature, *J. Mater. Civ. Eng.* 10 (1998) 58–64.
- [26] F. Ali, Is high strength concrete more susceptible to explosive spalling than normal strength concrete in fire? *Fire Mater.* 26 (2002) 127–130.
- [27] Recommendation of RILEM TC 200-HTC: mechanical concrete properties at high temperatures – modeling and applications, *Mater. Struct.* 40 (2007) 841–853.
- [28] G.F. Peng, Z.Sh. Huang, Change in microstructure of hardened cement paste subjected to elevated temperatures, *Constr. Build. Mater.* 22 (2008) 593–599.
- [29] J. Piasta, Z. Swicz, L. Rudzinski, Changes in the structure of hardened cement paste due to high temperature, *Mater. Struct.* 17 (1984) 291–296.
- [30] J. Dweck, P.M. Buchler, A.C. Vieira Coelho, F.K. Cartledge, Hydration of a Portland cement blended with calcium carbonate, *Thermochim. Acta* 346 (2000) 105–113.
- [31] N. Ukrainczyk, M. Ukrainczyk, J. Šipušić, T. Matusinović, XRD and TGA investigation of hardened cement paste degradation, in: 11th Conf. on Materials, Processes, Friction and Wear, MATRIB'06, Vela Luka, 2006, pp. 243–249.
- [32] E.T. Stepkowska, J.M. Blanes, F. Franco, C. Real, J.L. Pérez-Rodríguez, Phase transformation on heating of an aged cement paste, *Thermochim. Acta* 420 (2004) 79–87.
- [33] R. Gabrovšeka, T. Vukb, V. Kaučiča, Evaluation of the hydration of Portland cement containing various carbonates by means of thermal analysis, *Acta Chim. Slov.* 53 (2006) 159–165.
- [34] R. Vedalakshmi, A. Sundara Raj, S. Srinivasan, K. Ganesh Babu, Quantification of hydrated cement products of blended cements in low and medium strength concrete using TG and DTA technique, *Thermochim. Acta* 407 (2003) 49–60.